Int. J. Heat Mass Transfer. Vol. 21, pp. 275–284. Pergamon Press 1978. Printed in Great Britain

INFLUENCE OF THE PRANDTL NUMBER ON SECOND-ORDER HEAT TRANSFER DUE TO SURFACE CURVATURE AT A THREE-DIMENSIONAL STAGNATION POINT

KLAUS GERSTEN, HEINZ-D. PAPENFUSS and JOSEPH F. GROSS*
Institute for Thermo and Fluid Dynamics, Ruhr-University, Bochum, West Germany

(*Received* 22 *March* 1976 *and in revised form* 5 *January* 1977)

Abstract—The heat transfer at the stagnation point of a body in laminar, incompressible, three-dimensional flow is studied using second-order boundary-layer theory. The body is assumed to have two different principal curvatures at the stagnation point. The influence of the Prandtl number on the Nusselt number, in particular on the second-order terms resulting from longitudinal and transverse curvatures of the body surface, is shown. The conditions under which the contributions to the Nusselt number due to the transverse curvature effect and the longitudinal curvature effect cancel each other are demonstrated. Numerical results for a broad range of the Prandtl number ($0.2 \leqslant Pr \leqslant 12$) are given. The two limiting cases of very small and very large Prandtl numbers are considered using a perturbation analysis. Asymptotic expansions are obtained for both limiting cases; for very large Prandtl numbers, the method of matched asymptotic expansions is used to obtain the Nusselt number including both curvature effects. In the limiting case of very small Prandtl numbers, the first-order term for the Nusselt number, which is the result of Prandtl's boundary-layer theory, tends to zero as Prandtl numbers tend to zero. In contrast to this, the second-order contribution to the Nusselt number due to curvature approaches a finite, positive or negative value as Prandtl numbers tend to zero. Therefore, the second-order boundary-layer effect due to surface curvature gains significance in this case, and plays a key role for the heat transfer at stagnation points.

NOMENCLATURE

$A(\eta)$,	abbreviation, see equation (22);
B,	abbreviation, see equations (33) and (34);
c,	potential-flow parameter for three-dimensional stagnation points;
c_p,	specific heat of fluid;
D^*,	displacement thickness at stagnation point;
D_1, D_2, D_3,	linear differential operators, see equation (15);
f, F,	first- and second-order stream functions for stagnation-point flow;
g, G,	first- and second-order stream functions for stagnation-point flow;
h,	dimensionless first-order temperature;
K_{x0}, K_{z0},	principal curvatures at stagnation point, see Fig. 1;
Nu,	Nusselt number;
Pr,	Prandtl number, $Pr = \mu c_p/\lambda$;
Re,	Reynolds number;
St,	Stanton number;
T,	temperature;
T_∞,	temperature of oncoming flow;
u, v, w,	velocity components in the x, y and z-directions;
U_∞,	velocity of oncoming flow;
U_{11}, W_{11},	velocity gradients at stagnation point for the first-order potential flow;
U_{21}, W_{21},	velocity gradients at stagnation point for the second-order potential flow;
x, y, z,	orthogonal coordinates, origin at stagnation point, see Fig. 1.

Greek symbols

$\varepsilon, \varepsilon_1, \varepsilon_2$,	perturbation parameters;
ζ,	stretched normal variable, see equation (30);
η,	stretched normal variable, see equation (11);
θ,	dimensionless second-order temperature;
κ,	ratio of the two principle curvatures at stagnation point;
λ,	thermal conductivity of fluid;
μ,	viscosity of fluid;
ω,	abbreviation, related to the displacement thickness, see equations (16) and (18);
Ω,	constant in equation (24);
ρ,	density of fluid;
τ_{wx}, τ_{wz},	wall shear stresses in the x- and z-directions;
χ,	integral, see equation (17).

Subscripts

d, D,	displacement effect, proportional to U_{21} and W_{21}, respectively;
l,	longitudinal curvature;
t,	transverse curvature;
w,	wall;
st,	stagnation point.

*Department of Chemical Engineering, University of Arizona, Tucson, Arizona, U.S.A.

1. INTRODUCTION

SECOND-ORDER boundary-layer theory provides an extension of Prandtl's classical boundary-layer theory to moderate values of the Reynolds number. In incompressible flow, two effects become important when the Reynolds number is no longer large: (1) the displacement of the inviscid outer flow due to the presence of the boundary layer can not be neglected and (2) the curvature of the body surface must be taken into account. Other second-order effects appear when compressible flow is considered, see Van Dyke [1]. Much work has been done on higher-order boundary-layer theory and a review was recently given by Gersten and Gross [2].

Although classical boundary-layer theory was used for a broad range of technical problems involving heat transfer, the influence of the second-order effects on surface heat transfer has not been investigated extensively. Initial studies by Gersten and Gross [3] and Gersten [4] showed the influence of displacement and curvature effects together with the Prandtl number and wall mass transfer on the surface heat transfer. Their work is limited to incompressible stagnation-point flows for plane and axisymmetric bodies. The second-order effects for these particular flows were first considered by Van Dyke [5, 6].

Gersten and Gross [3] found that the surface curvature effect for the case of plane stagnation-point flow, where only longitudinal curvature is present, reduces the heat transfer for all values of the Prandtl number. For the case of axisymmetric stagnation-point flow, where both longitudinal and transverse curvature are present, Gersten [4] showed that the curvature effect leads to an increase in heat transfer for Prandtl numbers smaller than 11.352. When the Prandtl number is greater than 11.352, the curvature effect produces a decrease in the heat transfer. Gersten's work has been the first to show a change in the direction of the surface curvature effect with the Prandtl number when transverse curvature is present. We will consider in this work the following questions:

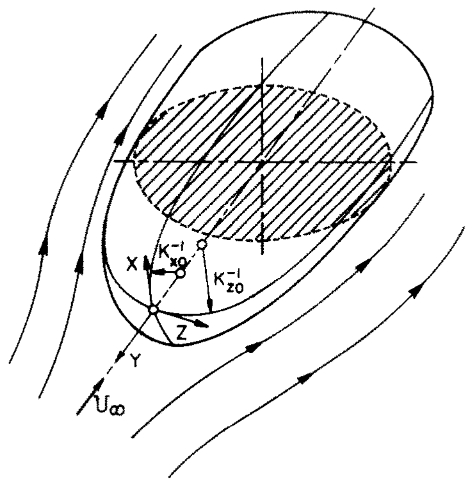

FIG. 1. Geometry and coordinate system.

(1) Under what conditions does the surface curvature increase or decrease the heat transfer when compared to the results of Prandtl's boundary-layer theory, and (2) under what conditions do the longitudinal and transverse curvature effects cancel each other?

We consider these problems for the relatively simple case of the three-dimensional stagnation-point flow with *two* principle curvatures (see Fig. 1), which will be interpreted here as longitudinal and transverse curvature. In particular, the question of how these two curvatures and the variation of the Prandtl number influence the heat transfer at the stagnation point will be studied. A consequence of this will be to establish the link between the investigations of plane [3] and axisymmetric [4] stagnation-point flows. In addition, this work provides an extension of the previous studies by Papenfuss [7–10] which deal with the second-order boundary-layer effects at three-dimensional stagnation points. That work, however, did not attempt to deal with a detailed discussion of the surface curvature effect on the heat transfer.

2. BASIC EQUATIONS

We consider the geometry of a general body in an incompressible flow as shown in Fig. 1. The ratio of the two principle curvatures at the stagnation point of the body is given by

$$\kappa = \frac{K_{z0}}{K_{x0}}. \tag{1}$$

The parameter κ may vary between $-\infty$ and $+\infty$; negative values denote geometrical saddle points. An orthogonal coordinate system is used, which consists of the lines of principal curvature at the body surface and the normals to the surface of the body.

To obtain the second-order boundary-layer equations for the three-dimensional flow from the Navier–Stokes equations, the *method of matched asymptotic expansions* has to be used. The solution of the problem described above can be expressed as an asymptotic expansion in the perturbation parameter ε

$$\varepsilon = (Re)^{-1/2} = \left(\frac{U_\infty \rho}{K_{x0}\mu}\right)^{-1/2} \tag{2}$$

in the region far from the wall (outer solution) and an asymptotic expansion for the region near the wall (inner solution). Outer and inner solutions are of the form

$$\phi = \phi_0 + \varepsilon\phi_1 + \varepsilon^2\phi_2 + \dots. \tag{3}$$

A stretched normal coordinate is used for the inner solution

$$\eta \sim \frac{y}{\varepsilon}. \tag{4}$$

The inner and outer solutions have to be matched properly in an overlapping domain of validity where the stretched "inner" variable η becomes very large, and the physical ("outer") variable y becomes very small. The approach is analogous to that described by Van Dyke [5] for the two-dimensional and axisymmetric flow.

The leading term of the outer expansion is the solution of the potential equation for the body. The second term of the outer expansion results from the displacement of the streamlines due to the presence of the boundary layer. This term is also obtained by the solution of the potential equation, with boundary conditions determined by matching with the first-order inner solution. This first-order inner solution (representing the leading term of the inner expansion) is identical with the solution of the Prandtl boundary-layer equations.

The second term of the inner expansion represents the solution of the so-called second-order boundary-layer equations, which are obtained by substituting expansions of the form shown in equation (3) into the Navier–Stokes equations and separating out terms of order ε. These equations take into account the effects due to surface curvature and boundary-layer displacement. In contrast to the first-order boundary-layer equations, the second-order boundary-layer equations are linear, so that the two second-order effects can be determined separately. A presentation of the first- and second-order boundary-layer equations will be omitted here for brevity; the details can be found in [9] or [10].

We will now, for simplicity, assume that the body has two planes of symmetry. Further, we restrict ourselves to flow symmetry. That is, the principal axes of flow at the stagnation point coincide with the directions of principal curvature of the body. Relaxation of these assumptions would result in additional second-order boundary-layer effects which are not considered here. For small distances from the stagnation point, the outer expansion of the velocities tangential to the wall is, to second-order,

$$\left.\begin{aligned} U(x) &= U_{11}x+\varepsilon U_{21}x+O(\varepsilon^2) \\ W(z) &= W_{11}z+\varepsilon W_{21}z+O(\varepsilon^2). \end{aligned}\right\} \tag{5}$$

The parameter c will be used in the subsequent analysis

$$c = \frac{W_{11}}{U_{11}} = \frac{(\mathrm{d}U/\mathrm{d}x)_{\mathrm{st},\varepsilon=0}}{(\mathrm{d}W/\mathrm{d}z)_{\mathrm{st},\varepsilon=0}} \tag{6}$$

which characterizes the deviation of the first-order potential flow at the stagnation point from the two-dimensional case ($c = 0$) and from the axisymmetric case ($c = 1$). In the present work, we restrict ourselves to values of the parameter c between 0 and 1. Possible negative values of c are not considered here; see Libby [11]. This restriction does not contradict the assumption made for the ratio of the two curvatures at the stagnation point. There exists no coupling between the parameter κ (which depends *only* on the geometry at the stagnation point) and the parameter c (which depends on the potential flow around the *entire* body).

Near the stagnation point, the velocity components in the x, y, and z-directions and the temperature of the boundary-layer flow may be expressed as follows:

$$\frac{u}{U_\infty} = U_{11}K_{x0}x\left\{f'(\eta)+\frac{\varepsilon}{\sqrt{U_{11}}}[F_l'(\eta)+\kappa(F_t'(\eta)-\eta f'(\eta))]+\frac{\varepsilon}{U_{11}}[U_{21}F_d'(\eta)+W_{21}F_D'(\eta)]\right\} \tag{7}$$

$$\begin{aligned}\frac{v}{U_\infty} = -\varepsilon\sqrt{U_{11}}\Big\{&f(\eta)+cg(\eta) \\ &+\frac{\varepsilon}{\sqrt{U_{11}}}[F_l(\eta)+cG_l(\eta)-\eta(f(\eta)+cg(\eta))+\kappa(F_t(\eta)+cG_t(\eta)-\eta(f(\eta)+cg(\eta)))] \\ &+\frac{\varepsilon}{U_{11}}[U_{21}(F_d(\eta)+cG_d(\eta))+W_{21}(F_D(\eta)+cG_D(\eta))]\Big\}\end{aligned} \tag{8}$$

$$\frac{w}{U_\infty} = W_{11}K_{x0}z\left\{g'(\eta)+\frac{\varepsilon}{\sqrt{U_{11}}}[G_l'(\eta)-\eta g'(\eta)+\kappa G_t'(\eta)]+\frac{\varepsilon}{U_{11}}[U_{21}G_d'(\eta)+W_{21}G_D'(\eta)]\right\} \tag{9}$$

$$\frac{T-T_w}{T_\infty-T_w} = h(\eta)+\frac{\varepsilon}{\sqrt{U_{11}}}[\theta_l(\eta)+\kappa\theta_t(\eta)]+\frac{\varepsilon}{U_{11}}[U_{21}\theta_d(\eta)+W_{21}\theta_D(\eta)]. \tag{10}$$

Dashes denote differentiation with respect to the stretched inner variable

$$\eta = K_{x0} y \frac{(U_{11})^{1/2}}{\varepsilon} = K_{x0} y (U_{11} Re)^{1/2}. \tag{11}$$

The subscripts l and t refer to the longitudinal and transverse curvature effect, respectively. The subscripts d and D refer to the displacement effect, proportional to U_{21} and W_{21}, respectively. In the following approach we consider only the curvature effect, the displacement effect has not been taken into account in the present work.

If we introduce equations (7)–(10) into the first- and second-order boundary-layer equations in [9] or [10], we obtain the following set of ordinary differential equations

$$\left.\begin{aligned} & f''' + (f+cg)f'' - (f'^2 - 1) = 0 \\ & D_1[F_l, G_l] = -\eta f''' + \eta(1-c) + \omega - c\chi + c\int_0^\eta (1 - f'g')\,d\eta \\ & D_1[F_t, G_t] = -\eta f''' + f'' + (f+cg)f' - 2\eta \end{aligned}\right\} \tag{12}$$

$$\left.\begin{aligned} & g''' + (f+cg)g'' - c(g'^2 - 1) = 0 \\ & D_2[F_l, G_l] = -\eta g''' + g'' + (f+cg)g' - 2c\eta \\ & D_2[F_t, G_t] = -\eta g''' - \eta(1-c) + \omega - \chi + \int_0^\eta (1 - f'g')\,d\eta \cdot \end{aligned}\right\} \tag{13}$$

$$\left.\begin{aligned} & h'' + Pr(f+cg)h' = 0 \\ & D_3[\theta_l] = h\{Pr[\eta(f+cg) - (F_l + cG_l)] - 1\} \\ & D_3[\theta_t] = h\{Pr[\eta(f+cg) - (F_t + cG_t)] - 1\}. \end{aligned}\right\} \tag{14}$$

The boundary conditions are

$$\begin{array}{ll} \eta = 0: & \eta \to \infty: \\ f = f' = g = g' = h = 0 & f' = g' = h = 1 \\ F_l = F_l' = G_l = G_l' = \theta_l = 0 & F_l'' = G_t'' = -1, G_l'' = F_t'' = 1 \\ F_t = F_t' = G_t = G_t' = \theta_t = 0 & \theta_l = \theta_t = 0. \end{array}$$

In equations (12)–(14) the following abbreviations have been used:

$$\left.\begin{aligned} & D_1[F, G] = F''' + (f+cg)F'' - 2f'F' + (F+cG)f'' \\ & D_2[F, G] = G''' + (f+cg)G'' - 2cg'G' + (F+cG)g'' \\ & D_3[\theta] = \theta'' + Pr(f+cg)\theta'. \end{aligned}\right\} \tag{15}$$

$$\omega = \lim_{\eta \to \infty} [(\eta - f) + c(\eta - g)] \tag{16}$$

$$\chi = \int_0^\infty (1 - f'g')\,d\eta. \tag{17}$$

The quantity ω is connected with the displacement thickness D^* at the stagnation point by the expression

$$D^* = \frac{\varepsilon}{\sqrt{U_{11}}} \frac{\omega}{1+c}. \tag{18}$$

From the solutions of the system of equations (12)–(14), we can determine the wall-shear stresses in the x- and z-direction and the Nusselt number, including the second-order terms due only to longitudinal and transverse curvature

$$\left.\begin{aligned} & \frac{\tau_{wx}}{\rho U_\infty^2} = \varepsilon U_{11}^{3/2} x \left[f_w'' + \frac{\varepsilon}{\sqrt{U_{11}}} (F_{lw}'' + \kappa F_{tw}'') \right] + O(\varepsilon^3) \\ & \frac{\tau_{wz}}{\rho U_\infty^2} = \varepsilon U_{11}^{3/2} cz \left[g_w'' + \frac{\varepsilon}{\sqrt{U_{11}}} (G_{lw}'' + \kappa G_{tw}'') \right] + O(\varepsilon^3) \end{aligned}\right\} \tag{19}$$

$$\frac{Nu}{\sqrt{Re}} = \sqrt{U_{11}} \left[h_w' + \frac{\varepsilon}{\sqrt{U_{11}}} (\theta_{lw}' + \kappa \theta_{tw}') \right] + O(\varepsilon^2) \tag{20}$$

with

$$Nu = \frac{1}{K_{x0}(T_\infty - T_w)} \left(\frac{dT}{dy} \right)_w. \tag{21}$$

The wall gradients, appearing in equation (20), may be derived from equations (14) by integration

$$h'_w = \frac{1}{\int_0^\infty e^{A(\eta)}\,d\eta}, \qquad A(\eta) = -Pr\int_0^\eta (f+cg)\,d\eta \tag{22}$$

$$\frac{\theta'_{lw}}{h'_w} = -\int_0^\infty \left\{ e^{A(\eta)} \int_0^\eta [Pr\eta(f+cg)-1-Pr(F_l+cG_l)]h\,e^{-A(\eta)}\,d\eta \right\} d\eta. \tag{23}$$

We obtain an analogous expression for θ'_{tw}, if we replace the subscript l in equation (23) everywhere by the subscript t.Numerical values for the wall gradients f''_w, g''_w, F''_{lw}, G''_{lw}, F''_{tw}, and G''_{tw} of the solutions of the systems (12) and (13) have been obtained for a range of the parameter c varying between 0 and 1. These values and the quantities ω and χ are given in Tables 1 and 2.

Table 1. Values for the wall gradients f''_w and g''_w and for ω and χ

c	f''_w	g''_w	ω	χ
0.00	1.23259	0.57047	0.64790	1.21837
0.25	1.24761	0.80514	0.83734	1.05418
0.50	1.26687	0.99811	0.96449	0.94898
0.75	1.28863	1.16432	1.06019	0.87400
1.00	1.31194	1.31194	1.13780	0.81658

Table 2. Values for the wall gradients F''_{lw}, G''_{lw}, F''_{tw} and G''_{tw}

C	F''_{lw}	G''_{lw}	F''_{tw}	G''_{tw}
0.00	−1.91326	−0.16018	0.54663	−0.66976
0.25	−1.84703	0.13269	0.50908	−1.18103
0.50	−1.77224	0.26776	0.46621	−1.42029
0.75	−1.69945	0.34148	0.42486	−1.55145
1.00	−1.63196	0.38676	0.38676	−1.63196

The intention of this work is to present numerical solutions to the system of equations (12)–(14) for a broad range of the Prandtl number and several values of the parameter c. The results for the wall gradients h'_w, θ'_{lw}, and θ'_{tw} are given in Table 3 and in Fig. 1.

Table 3. Wall gradients to determine the Nusselt number from equation (20) for the three-dimensional stagnation-point flow

	$c = 0$			$c = 0.25$			$c = 0.5$		
Pr	h'_w	θ'_{lw}	θ'_{tw}	h'_w	θ'_{lw}	θ'_{tw}	h'_w	θ'_{lw}	θ'_{tw}
0.2	0.296357	−0.053232	0.460715	0.323563	0.037555	0.364766	0.351182	0.107165	0.292742
0.4	0.395765	−0.088104	0.475010	0.429802	0.005808	0.372593	0.465474	0.082362	0.292027
0.7	0.495866	−0.128114	0.489863	0.536212	−0.030194	0.380155	0.579670	0.054070	0.290231
1.0	0.570465	−0.160182	0.501092	0.615277	−0.058776	0.385588	0.664396	0.031552	0.288389
2.0	0.743721	−0.239436	0.527361	0.798471	−0.128645	0.397602	0.860449	−0.023595	0.282980
4.0	0.961871	−0.344659	0.560441	1.028742	−0.220323	0.411754	1.106614	−0.096056	0.274734
7.0	1.178375	−0.452095	0.593122	1.257134	−0.313203	0.425037	1.350641	−0.169521	0.265617
10.0	1.338797	−0.532755	0.617240	1.426340	−0.382648	0.434537	1.531393	−0.224467	0.258482
11.0	1.384967	−0.556082	0.624167	1.475038	−0.402698	0.437229	1.583410	−0.240333	0.256384
11.35	1.400461	−0.563919	0.626491	1.491380	−0.409432	0.438129	1.600866	−0.245662	0.255677
12.0	1.428408	−0.578067	0.630681	1.520857	−0.421584	0.439748	1.632351	−0.255279	0.254395

	$c = 0.75$			$c = 1$		
Pr	h'_w	θ'_{lw}	θ'_{tw}	h'_w	θ'_{lw}	θ'_{tw}
0.2	0.378044	0.159433	0.239538	0.403840	0.199378	0.199378
0.4	0.500674	0.141040	0.231790	0.534739	0.186236	0.186236
0.7	0.623085	0.119813	0.222274	0.665378	0.170789	0.170789
1.0	0.713852	0.102819	0.214421	0.762231	0.158309	0.158309
2.0	0.923773	0.060993	0.194585	0.986202	0.127349	0.127349
4.0	1.187224	0.005776	0.167763	1.267254	0.086173	0.086173
7.0	1.448323	−0.050375	0.140066	1.545780	0.044100	0.044100
10.0	1.641701	−0.092441	0.119139	1.752059	0.012495	0.012495
11.0	1.697349	−0.104597	0.113071	1.811419	0.003353	0.003353
11.35	1.716024	−0.108680	0.111030	1.831339	0.000280	0.000280
12.0	1.749706	−0.116049	0.107345	1.867269	−0.005265	−0.005265

3. ASYMPTOTIC EXPANSIONS FOR SMALL PRANDTL NUMBERS

In the case of very small Prandtl numbers, the thickness of the momentum boundary layer is small in comparison to the thermal boundary layer. This means, that asymptotic expansions of the functions $f+cg$,

$F_l + cG_l$ and $F_t + cG_t$ for large η may be used in equations (22) and (23). These asymptotic expansions are

$$\left.\begin{aligned} f+cg &\to (1+c)\left(\eta - \frac{\omega}{1+c}\right) \\ F_l+cg_l &\to \frac{c-1}{2}\left(\eta - \frac{\omega}{1+c}\right)^2 + \frac{c-1}{1+c}\,\omega\left(\eta - \frac{\omega}{1+c}\right) - \Omega_l \\ F_t+cG_t &\to \frac{1-c}{2}\left(\eta - \frac{\omega}{1+c}\right)^2 + \frac{1-c}{1+c}\,\omega\left(\eta - \frac{\omega}{1+c}\right) - \Omega_t. \end{aligned}\right\} \tag{24}$$

The constants Ω_l and Ω_t depend on c. Since they do not enter the asymptotic solution for θ'_{lw} and θ'_{tw} to the order presented below, a presentation of the specific values has been omitted.

To obtain the asymptotic expansions for the equations (22) and (23) for very small Prandtl numbers, a perturbation analysis can be developed with

$$\varepsilon_1 = \sqrt{Pr} \tag{25}$$

as a perturbation parameter. The asymptotic solutions are:

$$h'_w = \left[\frac{2(1+c)}{\pi}\right]^{1/2} Pr^{1/2} - \frac{2\omega}{\pi} Pr + O(Pr^{3/2}) \tag{26}$$

$$\theta'_{lw} = \frac{4c}{3(1+c)\pi} + \left(1 - \frac{4}{3\pi}\right)\left[\frac{2(1+c)}{\pi}\right]^{1/2} c\,\omega\, Pr^{1/2} + O(Pr) \tag{27}$$

$$\theta'_{tw} = \frac{1}{c}\,\theta'_{lw}. \tag{28}$$

For $c = 0$ and $c = 1$ the results reduce to those given by Gersten and Gross [3] and Gersten [4]. It is worth mentioning that the result for h'_w and $c = 0$ has already been presented by Merk [10].

4. ASYMPTOTIC EXPANSIONS FOR LARGE PRANDTL NUMBERS

In the case of very large Prandtl numbers, $Pr \to \infty$, the thickness of the thermal boundary layer is very small in comparison to that of the momentum boundary layer. In this limiting case, the highest derivatives in the system of equation (14) vanish, leading to a singular perturbation problem. This problem can be solved by matching outer and inner solutions, which have to be expanded using the perturbation parameter

$$\varepsilon_2 = \frac{1}{(Pr)^{1/3}}. \tag{29}$$

For $Pr \to \infty$ we obtain an outer solution from equation (14) for the first-order temperature $h(\eta)$, which satisfies the boundary condition $h(\infty) = 1$; i.e. the trivial solution.

The inner solution, which has to link the outer solution and the prescribed boundary condition at the wall, is obtained by introducing a new stretched variable

$$\zeta = \frac{\eta}{\varepsilon_2} = \eta(Pr)^{1/3}. \tag{30}$$

For the functions f and g, which appear in equation (14), we may use a Taylor-series, expanded for small η; see also Merk [13]. After appropriate analysis, which also has to be applied to the second-order temperatures θ_l and θ_t, the following asymptotic expansions for the wall gradients are obtained

$$h'_w = \frac{3(f''_w + cg''_w)^{1/3}}{6^{1/3}\Gamma(1/3)} Pr^{1/3} - \frac{1}{2}\frac{\Gamma(2/3)}{\Gamma^2(1/3)}\frac{1+c^2}{f''_w + cg''_w} + O(Pr^{-1/3}) \tag{31}$$

$$\theta'_{lw} = \frac{1}{6^{1/3}\Gamma(1/3)}\frac{F'''_{lw} + cG'''_{lw}}{(f''_w + cg''_w)^{2/3}} Pr^{1/3} + \frac{\Gamma(2/3)}{\Gamma^2(1/3)}\left[\frac{1+c^2}{2}\cdot\frac{F'''_{lw} + cG'''_{lw}}{(f''_w + cg''_w)^2} + \frac{B_l}{2(f''_w + cg''_w)} + \frac{3}{2}\right] + O(Pr^{-1/3}) \tag{32}$$

$$B_l = \omega - c\chi + cg''_w. \tag{33}$$

The equation for θ'_{tw} is analogous to equation (32), if we replace the subscript l by the subscript t. Further, in this case, the expression for B_t is

$$B_t = c(\omega - \chi) + f''_w. \tag{34}$$

The two terms in equation (31) have already been reported by Merk [13] and Evans [14] for $c = 0$. For $c = 0$ and $c = 1$, equation (32) agrees with those given by Gersten and Gross [3] and Gersten [4].

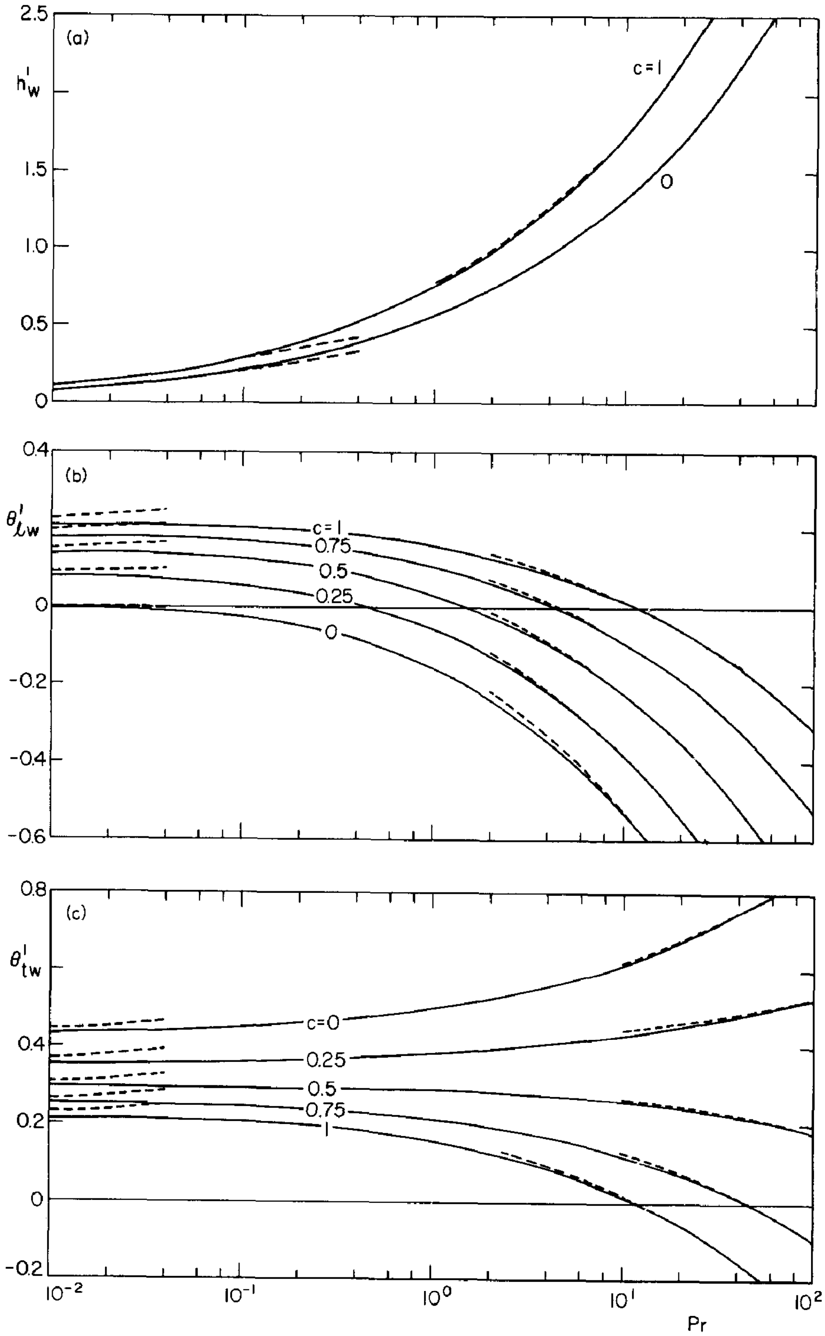

FIG. 2. Wall gradients to determine the Nusselt number from equation (20) for the three-dimensional stagnation-point flow. ---, asymptotic expansion.

5. DISCUSSION

Figures 2(a–c) show the first-order term for the Nusselt number, h'_w, and the second-order terms due to longitudinal and transverse curvature, θ'_{lw} and θ'_{tw}, respectively. The results are shown as functions of the Prandtl number in a range from 0.01 to 100 for various values of the parameter c. Both the numerical solutions as well as the asymptotic expansions for low and high Prandtl numbers are shown. The following conclusions can be made:

(1) The first order results, shown in Fig. 2(a), demonstrate the well-known effect of increasing Nusselt number with increasing Prandtl number for all values of c. For very small Prandtl numbers the first-order term for the Nusselt number approaches zero. The asymptotic expansion for large Prandtl numbers can not be shown for $c = 0$, because, in the scale of Fig. 2(a), it can not be distinguished from the exact results down to a Prandtl number of 0.1.

(2) The second-order contribution to the Nusselt number due to longitudinal curvature θ'_{lw} is shown in Fig. 2(b). For small Prandtl numbers, this contribution approaches finite positive values, except for $c = 0$, where θ'_{lw} tends to zero. For all values $c > 0$, θ'_{lw} crosses the abscissa at certain critical Prandtl numbers. For Prandtl numbers larger than these critical values, the

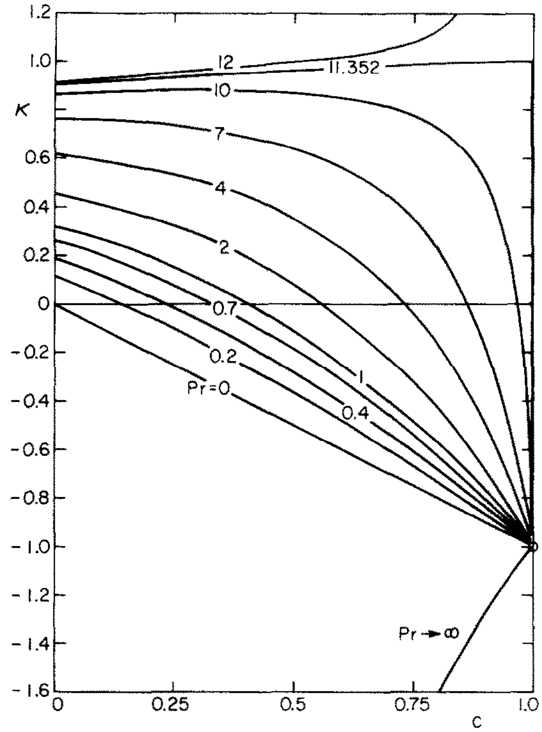

FIG. 3. Combinations of the parameters κ and c, for which the second-order term for the Nusselt number due to curvature vanishes.

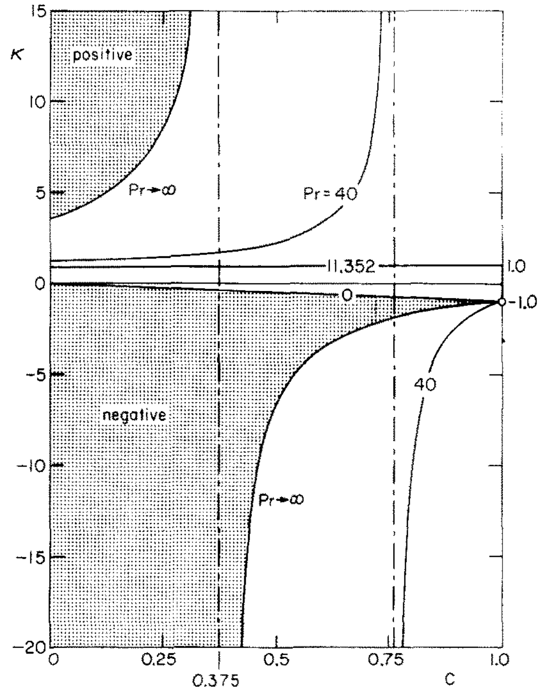

FIG. 4. Combinations of the parameters κ and c, for which the second-order term for the Nusselt number due to curvature vanishes.

contribution of the longitudinal curvature to the Nusselt number is negative. Only for $c = 0$ is this contribution negative for all Prandtl numbers. For large Prandtl numbers, θ'_{lw} tends to minus infinity.

(3) The second-order contribution to the Nusselt number due to transverse curvature θ'_{tw} is shown in Fig. 2(c). For small Prandtl numbers, this contribution approaches finite positive values. For $0 \leqslant c < 0.375$, the transverse curvature effect on the Nusselt number increases with increasing Prandtl numbers, whereas for $0.375 < c \leqslant 1$ this effect decreases with increasing Prandtl numbers (except for very low Prandtl numbers).

(4) According to equation (20), the total curvature effect, including longitudinal as well as transverse curvature, is proportional to $\theta'_{lw} + \kappa\theta'_{tw}$. This sum can be positive or negative, depending on the values of c, Pr and κ. The following example may illustrate this fact. We consider two convex bodies with $\kappa = 10$ in a flow with $Pr = 40$. The potential flow around two bodies may result in c-values of 0.5 and 0.75, respectively. From the asymptotic expansions for large Prandtl numbers, we obtain the following results:

$$c = 0.5: \quad \theta'_{lw} + \kappa\theta'_{tw} = 1.732$$

$$c = 0.75: \quad \theta'_{lw} + \kappa\theta'_{tw} = -0.197.$$

(5) Combinations of κ, c and Pr can be determined such that the total contribution of curvature is equal to zero, i.e. the contribution due to transverse curvature cancels that due to longitudinal curvature. In this case, we obtain

$$\kappa = -\frac{\theta'_{lw}}{\theta'_{tw}}.$$

Figure 3 shows this particular value of κ as a function of c with the Prandtl number as parameter. The curves begin at finite positive values on the κ-axis and all terminate at $c = 1$ and $\kappa = -1$. For $Pr = 11.352$, the c-curve has a discontinuity (kink) at $c = 1$, $\kappa = 1$.

For $Pr > 11.352$ the behavior of the curves changes completely. As is shown in Fig. 4, the results jump from $+\infty$ to $-\infty$ at a certain value c^*, depending on the Prandtl number. The curves for $Pr \to \infty$ and $Pr = 40$ are based on the asymptotic expansion (32).

It is worth mentioning that attempts to solve the system of equations (12)–(14) numerically would be very difficult for $Pr \gg 12$. For these values of the Prandtl number, the scale of the thermal boundary layer is so small in comparison to the momentum boundary layer, that the number of mesh points has to be extremely high to achieve meaningful results. Consequently, a perturbation analysis as in the present work is required to overcome this difficulty.

Two shaded areas can be seen in Fig. 4. The upper area contains those combinations of κ and c (e.g. $\kappa = 10$, $c = 0.1$) for which the effect due to transverse curvature is not sufficient to cancel the effect due to longitudinal curvature. Regardless of the value of the Prandtl number, the overall curvature effect then yields a positive contribution to the Nusselt number. On the other hand, the lower shaded area contains those combinations of κ and c (e.g. $\kappa = -10$, $c = 0.1$) for which the curvature effect reduces the Nusselt number, regardless of the Prandtl number. The dependence of the critical value c^* on the Prandtl number is shown in Fig. 5.

From the results for the Nusselt number, the

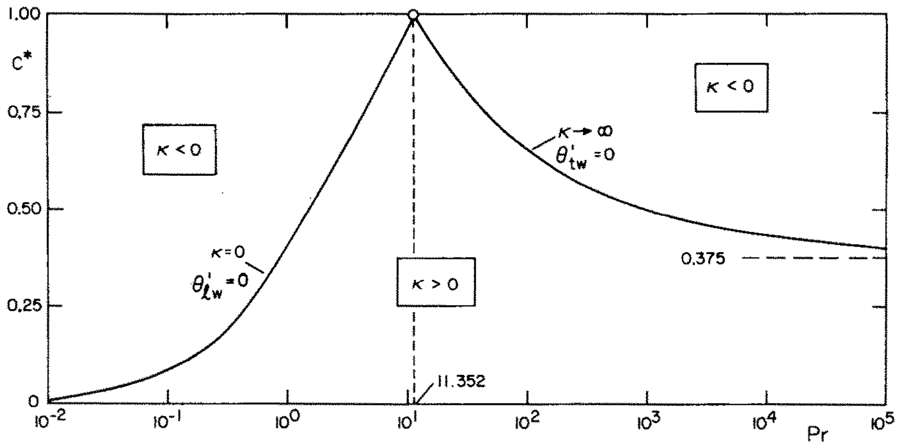

FIG. 5. Critical values of the parameter c as a function of the Prandtl number.

dimensionless heat transfer, expressed as the Stanton number, can be determined:

$$St = \frac{Nu}{RePr}. \tag{35}$$

A peculiarity occurs when we introduce the expansions for $Pr \to 0$ into equations (20) and (35):

$$St = \frac{\varepsilon}{\sqrt{Pr}}\left\{\left[\left(\frac{2(1+c)}{\pi}\right)^{1/2} - \frac{2\omega}{\pi}\sqrt{Pr} + O(Pr)\right]\sqrt{U_{11}} + \frac{\varepsilon}{\sqrt{Pr}}(c+\kappa)\left[\frac{4}{3(1+c)\pi} + \left[\left(1-\frac{4}{3\pi}\right)\left(\frac{2(1+c)}{\pi}\right)^{1/2}\omega\sqrt{Pr} + O(Pr)\right]\right\} + O\left[\left(\frac{\varepsilon}{\sqrt{Pr}}\right)^3\right]. \tag{36}$$

This asymptotic expansion is only valid if the second-order term is an order of magnitude smaller than the first-order term. Since the second-order term is multiplied by $\varepsilon/(Pr)^{1/2}$, ε must approach zero faster than $(Pr)^{1/2}$. In other words, we must require that

$$\lim_{Pr \to 0} \frac{\varepsilon}{(Pr)^{1/2}} \to 0. \tag{37}$$

It follows from equation (36) that the heat transfer tends to zero for $Pr \to 0$.

REFERENCES

1. M. Van Dyke, Second-order compressible boundary-layer theory with application to blunt bodies in hypersonic flow, in *Hypersonic Flow Research*, edited by F. R. Riddell, Vol. 7, pp. 37–76. Academic Press, New York (1962).
2. K. Gersten and J. F. Gross, Higher-order boundary-layer theory, in *Fluid Dynamics Transactions*, edited by W. Fiszdon, Vol. 7, part 2. Warszawa (1976).
3. K. Gersten and J. F. Gross, The effect of Prandtl number on second-order heat transfer, in *Proceedings of the Fifth International Heat Transfer Conference*, FC 2.2, pp. 55–59, Tokyo (1974).
4. K. Gersten, Effect of Prandtl number on second-order heat transfer at an axisymmetric stagnation point, to be published.
5. M. Van Dyke, Higher approximations in boundary-layer theory. Part I: general analysis, *J. Fluid Mech.* **14**, 161–177 (1962).
6. M. Van Dyke, Higher approximations in boundary-layer theory. Part 2: application to leading edges, *J. Fluid Mech.* **14**, 481–495 (1962).
7. H.-D. Papenfuss, Higher-order solutions for incompressible three-dimensional boundary-layer flow at the stagnation point of a general body, *Archwm Mech. Srosow.* **26**(6), 459–478 (1974).
8. H.-D. Papenfuss, Mass-transfer effects on the three-dimensional second-order boundary-layer flow at the stagnation point of blunt bodies, *Mech. Res. Commun.* **1**, 285–290 (1974).
9. H.-D. Papenfuss, Die Grenzschichteffekte 2. Ordnung bei der kompressiblen dreidimensionalen Staupunktströmung, Doctoral dissertation, University of Bochum, West-Germany (1975).
10. H.-D. Papenfuss, The second-order boundary-layer effects for the compressible three-dimensional stagnation-point flow, AIAA Paper No. 76-338 (1976).
11. P. A. Libby, Heat and mass transfer at a general three-dimensional stagnation point, *AIAA Jl* **5**, 507–517 (1967).
12. H. J. Merk, Rapid calculations for boundary-layer transfer using wedge solutions and asymptotic expansions, *J. Fluid Mech.* **5**, 460–480 (1959).
13. K. Gersten, Wärme- und Stoffübertragung bei grossen Prandtl-bzw. Schmidtzahlen, *Wärme- und Stoffübertragung* **7**, 65–70 (1974).
14. H. L. Evans, Mass transfer through laminar boundary layers—7. Further similar solutions to the b-equation for the case $B = 0$, *Int. J. Heat Mass Transfer* **5**, 35–57 (1962).

INFLUENCE DU NOMBRE DE PRANDTL SUR LE TRANSFERT THERMIQUE AU POINT D'ARRET POUR UNE SURFACE TRIDIMENSIONNELLE

Résumé—Le transfert thermique au point d'arrêt d'un corps pour un écoulement laminaire, incompressible et tridimensionnel est étudié en utilisant la théorie au second ordre de la couche limite. On suppose que le corps à deux courbures principales différentes au point d'arrêt. On montre l'influence du nombre de Prandtl sur le nombre de Nusselt, en particulier sur les termes de second ordre résultat des courbures longitudinale et transversale sur la surface du corps. On précise les conditions pour lesquelles les contributions de l'effet des courbures s'annulent. On donne des résultats numériques pour un large domaine de nombre de Prandtl ($0,2 < \mathrm{Pr} < 12$). Les deux cas limites des très petits et des très grands nombres de Prandtl sont considérés à travers l'analyse de perturbation. On obtient des développements asymptotiques pour ces deux cas; pour les très grands nombres de Prandtl, la méthode des développements asymptotiques est utilisée pour obtenir le nombre de Nusselt en incluant les effets de la courbure. Dans le cas des très petits nombres de Prandtl, le terme du premier ordre pour le nombre de Nusselt (qui est le résultat de la théorie de la couche limite selon Prandtl) tend vers zéro quand le nombre de Prandtl s'approche de zéro; par contre la contribution de second ordre au nombre de Nusselt par l'effet de courbure tend vers une valeur finie, positive ou négative lorsque le nombre de Prandtl tend vers zéro. Par suite, l'effet dû à la courbure de surface est significatif dans ce cas et joue un rôle important dans le transfert thermique au point d'arrêt.

DER EINFLUSS DER PRANDTL-ZAHL AUF DEN WÄRMEÜBERGANG ZWEITER ORDNUNG INFOLGE DER OBERFLÄCHENKRÜMMUNG IM STAUPUNKT

Zusammenfassung—Der Wärmeübergang im Staupunkt eines Körpers wird unter Berücksichtigung der Glieder höherer Ordnung der Grenzschichtgleichungen für laminare, inkompressible und dreidimensionale Strömung untersucht. Für den Körper werden zwei verschiedene Krümmungen im Staupunkt angenommen. Der Einfluß der *Pr*-Zahl auf die *Nu*-Zahl, speziell auf die Glieder zweiter Ordnung als Folge der Längs- und Querkrümmung der Körperoberfläche wird dargestellt. Es wird gezeigt, unter welchen Bedingungen sich die Einflüsse von Längs- und Querkrümmung auf die Nu-Zahl gegenseitig aufheben. Für einen weiten Bereich der *Pr*-Zahl ($0,2 \leqq Pr \leqq 1,2$) werden Zahlenergebnisse mitgeteilt. Die Grenzfälle der sehr kleinen und sehr großen *Pr*-Zahl werden im Rahmen einer Störanalyse betrachtet. Für beide Fälle erhält man asymptotische Grenzwerte: Für sehr große *Pr*-Zahlen liefert die Reihenentwicklung die von beiden Krümmungen beeinflußte *Nu*-Zahl. Für Grenzfall der sehr kleinen *Pr*-Zahl geht der Term erster Ordnung für die *Nu*-Zahl, der sich aus der Grenzschichttheorie Prandtls ergibt, gegen Null. Im Gegensatz hierzu nimmt das Glied zweiter Ordnung, welches die Krümmung berücksichtigt, einen endlichen positiven oder negativen Wert an, wenn die *Pr*-Zahl gegen Null geht. Der Grenzschichteffekt zweiter Ordnung gewinnt in diesem Fall an Bedeutung und nimmt eine Schlüsselrolle beim Wärmeübergang im Staupunkt ein.

ВЛИЯНИЕ ЧИСЛА ПРАНДТЛЯ НА ТЕПЛООБМЕН ВТОРОГО ПОРЯДКА, ОБУСЛОВЛЕННОЕ КРИВИЗНОЙ ПОВЕРХНОСТИ В ТРЕХМЕРНОЙ КРИТИЧЕСКОЙ ТОЧКЕ

Аннотация — С помощью теории пограничного слоя второго порядка изучается теплообмен в критической точке тела в ламинарном, трехмерном потоке несжимаемой жидкости. Предполагается, что тело в критической точке имеет две различные главные кривизны. Показано влияние числа Прандтля на число Нуссельта, в частности, на вклады второго порядка, обусловленные продольной и поперечной кривизнами поверхности тела. Рассматриваются условия, при которых вклады в число Нуссельта, обусловленные поперечной и продольной кривизнами, взаимно уничтожаются. Приводятся численные результаты для широкого диапазона числа Прандтля ($0.2 \leq Pr \leq 12$). С помощью теории возмущений анализируются два предельных случая малых и больших чисел Прандтля. Для обоих предельных случаев получены асимптотические разложения; при больших числах Прандтля для получения чисел Нуссельта, с учетом обоих вкладов кривизны, используется метод сращиваемых асимптот. В предельном случае малых чисел Прандтля вклад первого порядка в число Нуссельта, определяемого теорией пограничного слоя Прандтля, стремится к нулю вместе с числом Прандтля. В отличие от этого, вклад второго порядка в число Нуссельта, обусловленный кривизной приближается к конечному положительному или отрицательному значению, по мере того как число Прандтля стремится к нулю. Вследствие этого эффект пограничного слоя второго порядка, обусловленный кривизной, поверхности, приобретает важное значение и играет основную роль в теплообмене в критических точках.